



Rosmarinic acid and its derivative's duel as antitubercular agents: insights from computational prediction to functional response *in vitro*

Nandan Sarkar, Pukar Khanal, Ravi Rawat, Yadu Nandan Dey & Kuldeep K. Roy

To cite this article: Nandan Sarkar, Pukar Khanal, Ravi Rawat, Yadu Nandan Dey & Kuldeep K. Roy (2024) Rosmarinic acid and its derivative's duel as antitubercular agents: insights from computational prediction to functional response *in vitro*, Journal of Biomolecular Structure and Dynamics, 42:23, 12720-12729, DOI: [10.1080/07391102.2023.2272754](https://doi.org/10.1080/07391102.2023.2272754)

To link to this article: <https://doi.org/10.1080/07391102.2023.2272754>



Published online: 25 Oct 2023.



Submit your article to this journal [↗](#)



Article views: 105



View related articles [↗](#)



View Crossmark data [↗](#)



Citing articles: 1 View citing articles [↗](#)



Rosmarinic acid and its derivative's duel as antitubercular agents: insights from computational prediction to functional response *in vitro*

Nandan Sarkar^a , Pukar Khanal^{b,c} , Ravi Rawat^d , Yadu Nandan Dey^e  and Kuldeep K. Roy^d 

^aDepartment of Pharmaceutical Technology, School of Health and Medical Science, Adamas University, Kolkata, West Bengal, India;

^bDepartment of Pharmacology and Toxicology, KLE College of Pharmacy Belagavi, KLE Academy of Higher Education and Research (KAHER) Belagavi, Belagavi, India; ^cDepartment of Pharmacology, Nitte Gulabi Shetty Memorial Institute of Pharmaceutical Sciences (NGSMIPS), NITTE University, Mangalore, India; ^dDepartment of Pharmaceutical Sciences, School of Health Sciences and Technology, UPES University, Dehradun, Uttarakhand, India; ^eDepartment of Pharmacology, Dr. B.C. Roy College of Pharmacy and Allied Health Sciences, Durgapur, West Bengal, India

Communicated by Ramaswamy H. Sarma

ABSTRACT

Tuberculosis is one of the most dreadful infectious diseases, afflicting global populations with anguish. With the emergence of multi-drug resistant strains of mycobacteria, the imperative for new anti-tuberculosis drugs has grown exponentially. Thus, the current study delves into evaluating the impact of *Perovskia abrotanoides* and its active metabolites-namely, rosmarinic acid and its derivatives-against strains of *Mycobacterium tuberculosis* (Mtb). Through the use of the CRI assay, the antimycobacterial potential of the high-altitude medicinal plant *P. abrotanoides* was gauged, while docking and molecular dynamics simulations unveiled plausible targets. Of these, the peak antimycobacterial effectiveness was observed in the *P. abrotanoides* ethyl acetate extract with 125 µg/mL as minimum inhibitory concentration against various strains of *M. tuberculosis*, encompassing H37Rv and strains resistant to multiple drugs. Following bioassay-guided fractionation and isolation, rosmarinic acid and rosmarinic acid methyl ester emerged as potent molecules against H37Rv and multidrug-resistant *M. tuberculosis* strains; minimum inhibitory concentration ranging from 15 to 32 µg/mL. Additionally, out of 22 targets explored, Mtb lipamide dehydrogenase (PDB: 3II4) and Rv2623 (PDB: 3CIS) were forecasted as potential Mtb targets for rosmarinic acid and rosmarinic acid methyl ester, respectively, a supposition further affirmed by molecular simulations (100 ns). The stability of both complexes throughout the simulation was measured by protein backbone root-mean-square deviation, substantiating their roles as respective targets for antimycobacterial activities.

ARTICLE HISTORY

Received 14 September 2022
Accepted 17 September 2023

KEYWORDS







Perovskia abrotanoides;
rosmarinic acid;
tuberculosis; molecular
docking; molecular
dynamics

1. Introduction

Tuberculosis stands as one of the most formidable infectious diseases, afflicting approximately 10.4 million individuals and resulting in 1.8 million deaths annually. This bacterial infection is primarily caused by *Mycobacterium tuberculosis*. As per the World Health Organization's report, tuberculosis affects roughly 30% of the global population and contributes to 3 million annual deaths worldwide (Bloom et al., 2017). The contemporary treatment of tuberculosis faces significant obstacles due to the emergence of drug-resistant strains of *Mycobacterium*. The risk of contracting tuberculosis is notably elevated among individuals with diabetes and other chronic, debilitating diseases linked to compromised immune systems. Despite being a curable ailment, tuberculosis necessitates prolonged treatment spanning up to six months or more, entailing a combination of drugs that often entail numerous side effects. The widespread utilization of anti-tuberculosis medications has led to an escalating prevalence of resistance, extending beyond the frontline drugs, such as

isoniazid and rifampicin, to encompass an increasing array of second-line drugs. This has resulted in the emergence of multidrug-resistant (MDR) strains and extensively drug-resistant strains.

This situation brings us face-to-face with the urgent need for developing new drugs that are more potent, as well as new regimens that can shorten the treatment time, are inexpensive, safe, capable of tackling resistant strains, and can be used to provide effective treatment for non-replicative latent forms without interfering with antiretroviral therapy. Since the introduction of rifampicin over 50 years ago, most anti-tuberculosis drugs that have been developed are new formulations of existing agents. Plant-derived compounds have shown a drastic reduction in the growth of pathogens without inflicting any toxic effects on host cells (Kohl et al., 2019). Despite the great number of modern drugs obtained through total synthesis, natural products remain one of the main sources of novel chemical structures and drug candidates. Previous studies have revealed that some medicinal

CONTACT Nandan Sarkar  nandansarkar88@gmail.com  Department of Pharmaceutical Technology, School of Health and Medical Science, Adamas University, Kolkata-700126, West Bengal, India; Yadu Nandan Dey  yadunandan132@gmail.com; yadunandandey@gmail.com  Department of Pharmacology, Dr. B.C. Roy College of Pharmacy and Allied Health Sciences, Durgapur-713206, West Bengal, India; Kuldeep Kumar Roy  kuldeepkroy@gmail.com  Department of Pharmaceutical Sciences, School of Health Sciences and Technology, UPES, Dehradun-248007, Uttarakhand, India.

plants like *Semecarpus anacardium*, *Adhatoda vasica*, *Camchaya calcarea*, and *Zanthoxylum capense* for promising antimycobacterial activity. The various phytoconstituents like quinazoline alkaloids; vasicine and vasicinone isolated from *Justicia adhatoda*; pinocebrin, a flavanone from *Cryptocarya chinensis*; and a glycosyloxyflavone baicalin from *Scutellaria baicalensis* showed significant anti-mycobacterial activity (Chou et al., 2011; Ignacimuthu & Shanmugam, 2010; Zhang et al., 2017).

Perovskia abrotanoides is a small, aromatic, erect herb belonging to the Labiatae family, found in the mountains of Asian countries (Alizadeh et al., 2021) and used to treat atherosclerosis, cardiovascular diseases, liver fibrosis, and other diseases in traditional Chinese medicine (Beikmohammadi, 2012). In Iranian folk medicine, *P. abrotanoides* is also used for the treatment of leishmaniasis (Moghaddas et al., 2017). Previous studies carried out on this plant have revealed its leishmanicidal, anti-plasmodial, and cytotoxic activities. Earlier works on the isolation and identification of bioactive molecules have resulted in the isolation of tanshinones and two triterpenes with a novel carbon skeleton. However, no biological activity has been attributed to these compounds (Jiang et al., 2019). The oil of *P. abrotanoides* has been reported to have antimicrobial activity against *S. aureus*, *B. cereus*, *E. coli*, *A. niger*, and *C. albicans* (Mahboubi & Kazempour, 2009). Despite exhibiting various biological activities, no study has been carried out to examine its activity against clinical isolates of *M. tuberculosis*. Hence, in the present study, the antimycobacterial activity of various *P. abrotanoides* extracts or fractions and isolated pure compounds was evaluated using the Colorimetric Redox Indicator (CRI) assay.

Previously, many studies were conducted to gain insights into the mechanistic pathway of antitubercular activity which includes molecular docking analysis and simulation studies. In recent times, the use of molecular simulation for calculating molecular electronic structures, machine learning for predicting structural activities, and molecular mechanics for molecular modeling, alongside in-silico approaches in computer-aided drug design, has garnered tremendous attention and application. This approach has accelerated the discovery of novel compounds with ease, cutting research costs in terms of time, energy resources, and manpower (Owen et al., 2023).

Previously, rosmarinic acid and methyl rosmarinic acid were isolated and purified from the *Rosmarinus* species. Various biological evaluations were performed, including assessments against cancer, antibacterial effects, anti-inflammatory responses, neuroprotective actions, asthma treatment, and antioxidant properties (Fachel et al., 2019; Fazel Nabavi et al., 2015). Recently, it has been demonstrated that rosmarinic acid-containing extracts from *Melissa officinalis* have been effective against the *Herpes simplex* virus. rosmarinic acid has also exhibited potential against human immunodeficiency virus type-1 (Fazel Nabavi et al., 2015; Sedano-Partida et al., 2020). However, the potential antimycobactericidal efficacy of rosmarinic acid has not been evaluated. The present study assessed the antimycobacterial activity against both normal and MDR strains. The assay yielded promising results; however, due to the limited

quantity of compounds obtained from natural sources, in-vivo studies were not feasible. Consequently, computational studies were conducted to establish the efficacy and efficiency of the molecule against tuberculosis.

Computational methods have been successfully employed by researchers to evaluate the chemical properties of active biomolecules for multiple pharmacological spectra. Previously, the potential antioxidant properties of rosmarinic acid have been demonstrated through ground-state molecule's geometry analysis, free radical structure, characteristics of highest (occupied) and lowest (unoccupied) molecular orbital, required energy to break the hydroxyl bond, and pattern of electrons distribution in the radicals (Eno et al., 2022; Manicum et al., 2023). Molecular docking allows for a more precise prediction of binding site locations, docking poses, and the likelihood of binding affinity (Nandi et al., 2023; Patil et al., 2023; K. Wei et al., 2022). In the current study, to understand the mechanistic basis of biological action, a molecular docking study was executed, and potential targets were identified through docking analysis against 22 target proteins. The results showed promise against two proteins. Numerous molecular simulation studies are primarily conducted to observe biomolecular processes in action, particularly essential functional processes such as ligand binding, ligand- or voltage-induced conformational changes, protein folding, or membrane transport. Simulations are frequently employed to generate a qualitative understanding of how biomolecules or drugs function (Benjamin et al., 2022; Bhattacharya et al., 2023; Chattaraj et al., 2023). As a result, molecular simulation experiments were also performed with the current molecule to validate the stability, energetics, and thermodynamics of the target molecules.

2. Materials methods

2.1. Plant collection, authentication, and extraction

The whole plant of *Perovskia abrotanoides* was collected from Khardungla, Ladakh, India (altitudes ranging from 3000 m to 5200 m above sea level) during the months of July–August 2020. The collected plants were authenticated by Dr. S. Kitchlu from the Department of Botany, Council of Scientific & Industrial Research-Indian Institute of Integrative Medicine (CSIR-IIIM), and voucher specimens were deposited at the herbarium for the same in CSIR-IIIM in Jammu and the Chemical Biology Laboratory, J3 Block, AIB, AUUP, Noida.

The air-dried plant material (500 g) was finely ground and extracted using a mixture of MeOH: H₂O in a 4:1 ratio. In detail, the plant materials were soaked in a 1 L methanol-water (4:1) solvent system for 10 h at room temperature. Subsequently, they were filtered, and the residue was subjected to another round of soaking in the same solvent system. This process was repeated five times. The filtrate obtained was combined and then concentrated under reduced pressure at 40 °C. To safeguard against the degradation of thermolabile compounds, cold water at 4 °C was circulated during this process. The concentrated methanolic extract was suspended in water and then partitioned using a separating funnel with n-hexane. This partitioning procedure was carried out sequentially with dichloromethane and ethyl

acetate. The organic fractions thus obtained were collected and concentrated using a rotavapor. The remaining aqueous fraction was subjected to lyophilization, and the yields of the resulting dried fractions were documented.

2.2. Procurement of *M. tuberculosis* strains

M. tuberculosis pan-sensitive strain H37Rv, TMC-102 (sensitive to rifampicin, streptomycin, isoniazid, pyrazinamide, and ethambutol), and MDR clinical isolate (Tb-14,348/16), resistant to rifampicin and isoniazid were obtained from Dr. V.M. Katoch, National JALMA Institute of Leprosy and other Mycobacterial Diseases, Agra, India.

2.3. Antimycobacterial activity by CRI assay

The *in-vitro* antimycobacterial activity of the different *P. abrotanoides* extracts were performed using CRI assay against H37Rv and MDR strains of *M. tuberculosis* (Sarkar et al., 2018)). Briefly, to a 96-well microliter plate, 160 μ l of 7H9-S broth was added to all wells except for the outer periphery wells. A stock solution of the plant extracts (1 mg/mL) concentration was prepared using 1 mg extract dissolved in 1 mL sterile distilled water with 0.5 to 2% dimethyl sulphoxide (DMSO). To the first well, 40 μ l of the extract was added and two-fold serial dilution was performed. The extracts were dissolved in a maximum of 2% DMSO and were diluted with sterile distilled water to obtain final sample concentrations in the range of 1–0.0019 mg/mL. To avoid evaporation during incubation, sterile distilled water was added to all the outer wells. The plate was covered with the lid and sealed properly with parafilm from all sides and incubated at 37 °C for 5–7 days. Rifampicin was used as a positive control, media with bacterial suspension was considered as growth control, and 0.5% DMSO with media and bacterial suspension was used as DMSO control. After 5–6 days of the incubation period, 25 μ l of 0.02% freshly prepared resazurin was added to all the wells in plates and re-incubated overnight for the development of color. The color change from blue to pink interpreted the growth of bacteria at that concentration of the extract. The color was compared with the color in the growth control wells and the minimum inhibitory concentration (MIC) of each extract was determined as the lowest concentration of the extract that prevents a change in color of indicator dye resazurin where blue color is interpreted as an absence of mycobacterial growth and pink color indicates bacterial growth.

2.4. Bioactivity-guided fractionation and isolation of active compounds

After confirming the activity, the crude methanol extract of *P. abrotanoides* was subjected to successive silica gravity column chromatography with gradient elution with *n*-hexane and ethyl acetate (5% increment with ethyl acetate). Eight major fractions were obtained based on similarities in TLC profiles two potent active principle was identified based on bioassay-guided fractionation. Further Sephadex LH-20 gel

permeation chromatography was performed for purification. Final separation and purification by reverse phase semi-prep HPLC with methanol-water gradient elution resulted in the isolation of PA1 and PA2. Structural identification of active isolate was performed based on spectral analysis (¹H-, ¹³C-NMR, and MS data).

2.5. Computational chemistry

2.5.1. Ligand preparation

The 3D structure of rosmarinic acid and methyl-rosmarinic acid were obtained from PubChem (<https://pubchem.ncbi.nlm.nih.gov/>) database, the spatial data file(.sdf) form of the compounds was first retrieved, then using Discovery studio visualize 2019 these structures were converted into protein data bank (.pdb) and subjected to docking.

2.5.2. Target preparation

The 3D structure targets isocitrate lyase of *Mycobacterium tuberculosis* (PDB: 1F8M), AhpD of *Mycobacterium tuberculosis* (PDB:1KNC), aminoglycoside 2'-N-acetyltransferase of *Mycobacterium tuberculosis* A(PDB:1M4I), seca protein translocation ATPase (PDB:1NKT), MabA from *Mycobacterium tuberculosis* (PDB:1UZL), alanine racemase (PDB:1XFC), hypoxic response protein I (PDB:1XKF), Thioredoxin reductase (PDB:2A87), catalase-peroxidase (KatG) (PDB:2CCA), catalytic domain of protein kinase PknB from *Mycobacterium tuberculosis* (PDB:2FUM), Pribnow Box recognition region of SigC from *Mycobacterium tuberculosis* (PDB: 2O7G), Protein kinase PknG from *Mycobacterium tuberculosis* (PDB:2PZI), β -ketoacyl-acyl carrier protein synthase III (FABH) and decyl-COA disulphide (PDB:2QX1), KasA of *Mycobacterium tuberculosis* (PDB:2WGE), *Mycobacterium tuberculosis* hypoxic response regulator DosR (PDB:3C3W), Rv2623 from *Mycobacterium tuberculosis* (PDB:3CIS), Precorrin-6y C5,15-methyltransferase (PDB:3E05), mycobacterial lipoamide dehydrogenase (PDB:3II4), apo D-alanine:D-alanine Ligase (Ddl) from *Mycobacterium tuberculosis* (PDB:3LWB), C-terminal extracellular domain of *Mycobacterium tuberculosis* EmbC (PDB:3PTY), ICDH-1 from *Mycobacterium tuberculosis* (PDB:4HCX) and mycobacterial ATP synthase (PDB:4V1H) and dihydro lipoyldehydrogenase (PDB:3II4) were retrieved from Research Collaboratory for Structural Bioinformatics database (<https://www.rcsb.org/>). The retrieved protein structures were in a complex with water molecules and other hetero-atoms, which were removed using Discovery Studio 2019 and saved in .pdb format.

2.5.3. Ligand-protein docking

The prepared ligands were docked against the selected proteins as explained previously (Khanal et al., 2020, 2021). The docking study was performed with 22 targets and 2 ligands, i.e. rosmarinic acid and methyl-rosmarinic acid, the energy of ligand molecules was minimized using MMFF94 force field and then docking was performed using Auto Dock Vina. After the completion of docking, ten different poses were obtained, the pose with the best fit having the lowest

binding energy was selected and visualized in Discovery Studio 2019.

2.5.4. Molecular dynamics (MD) simulation

The MD simulation was carried out using GROMACS (Kumari et al., 2022; Pronk et al., 2013; Van Der Spoel et al., 2005). The MD system contained the ligand-bound protein model, POPC (1-palmitoyl-2-oleoyl-sn-glycero-3-phosphocholine) lipid layer, water (TIP3P), and ions (K^+ and Cl^-). The GROMOS96 43a1 was used as a force field for the building of the lipid-water system. To relieve the system from steric clashes and initial thermal fluctuation, the system was subjected to the equilibration run. The sufficient equilibration of the MD system was analyzed using plots of various parameters (such as potential energies, temperature, and protein-backbone RMSD) to time (ps). The equilibrated system was subjected to a production run (100 ns). The MD trajectory analysis was done using various tools integrated within GROMACS, HeroMDAnalysis (Rawat et al., 2021), and using VMD (Humphrey et al., 1996). The Grace tool was used to plot several graphs.

3. Results and discussion

3.1. Identification of compounds from *P. abrotanoides* that can serve as ideal leads for drug development against tuberculosis

Different *P. abrotanoides* extracts were screened for antimycobacterial activity against the H37Rv strain of *M. tuberculosis* including the MDR strains also (Table 1). Based on the results of the CRI assay, the ethyl acetate extract of *P. abrotanoides* showed maximum antimycobacterial activity against both the strains including H37Rv and MDR at 125 $\mu\text{g/mL}$ respectively. The CRI assay has the advantage of being simpler, faster, and less laborious. Natural products from various sources like plants and microorganisms have been screened for antimycobacterial activity using the CRI assay (Fernandes et al., 2021).

Among all the different fractions of *P. abrotanoides*, the ethyl acetate fractions exhibited maximal activity. Hence, the ethyl acetate extract of *P. abrotanoides* was selected for further isolation and characterization of active anti-tuberculosis molecules. Fractions were isolated and a bioassay of isolated fractions was performed against the clinical isolates (MDR and drug-sensitive) as well as the standard strain of *M. tuberculosis*, H37Rv strain using a CRI assay to identify the potent fractions. The antitubercular activity of the eight

fractions (Fr 1–Fr 8) eluted from column chromatography is shown in Table 2.

Among the eight fractions tested, fractions 3 (Fr 3) and 6 (Fr 6) showed significant activity against *M. tuberculosis* at a concentration of 31.25–62.50 $\mu\text{g/mL}$. Fractions 2 (FR-2) and five (FR-5) had moderate activity at a higher concentration of 62.5–250 $\mu\text{g/mL}$. Further isolation and purification of the active fraction 3 (Fr 3) and 6 (Fr 6) was accomplished using the Sephadex column and HPLC. The purified compounds were subjected to spectral analyses (NMR and Mass) and were characterized by comparing ^1H and ^{13}C NMR data with the reported literature data (Akoury, 2017; Serrano et al., 2021) and were unambiguously identified as methyl rosmarinic acid and rosmarinic acid (Figure 1).

Methyl rosmarinic acid: $\text{C}_{19}\text{H}_{18}\text{O}_8$; ESIMS (negative ion): m/z 373.33339 $[\text{M}-\text{H}]^-$ (calculated for 373.33348); $^1\text{H-NMR}$ (CD_3OD): δ 7.52 (1H, d, $J = 15.5$ Hz, H-7'), 7.04 (1H, d, $J = 2.0$ Hz, H-2'), 6.91 (H, dd, $J = 8.5, 2.0$ Hz, H-6'), 6.75 (1H, d, $J = 8.5$ Hz, H-5'), 6.71 (1H, d, $J = 2.0$ Hz, H-2), 6.64 (1H, d, $J = 8.0$ Hz, H-5), 6.61 (1H, dd, $J = 8.0, 2.0$ Hz, H-6), 6.27 (1H, d, $J = 15.5$ Hz, H-8'), 5.11 (1H, dd, $J = 7.5, 5.0$ Hz, H-8), 3.72 (3H, s, OCH_3), 3.06 (1H, dd, $J = 14.5, 5.5$ Hz, H-7a), 3.00 (1H, dd, $J = 14.5, 5.5$ Hz, H-7b); ^{13}C NMR (CD_3COCD_3 , 125 MHz): δ c 170.2 (C-9), 166.3 (C-9'), 148.2 (C-3 and C-3'), 146.2 (C-4'), 145.5 (C-7'), 144.6 (C-4), 143.6 (C-1), 129.2 (C-1'), 122.2 (C-6), 120.9 (C-6'), 116.8 (C-5 and C-5'), 115.6 (C-8'), 114.8 (C-2), 113.7 (C-2'), 73.3 (C-8), 51.6 (C-10), 31.2 (C-7).

Rosmarinic acid: $\text{C}_{18}\text{H}_{16}\text{O}_8$; ESIMS (negative ion) m/z 359.07597 $[\text{M}-\text{H}]^-$ (calculated for 359.07656); ^1H NMR (CD_3OD , 500 MHz): δ 7.36 (1H, d, $J = 16$ Hz, H-7'), 7.08 (1H, d, $J = 8.0$ Hz, H-5), 6.95 (br s, H-2), 6.88 (br d, $J = 8.0$ Hz, H-6), 6.87 (d, $J = 8.0$ Hz, H-5'), 6.78 (br s, H-2'), 6.75 (br d, $J = 8.0$ Hz, H-6'), 6.14 (d, $J = 16.0$ Hz, H-8'), 5.28 (dd, $J = 4.3$ Hz, and $J = 8.6$ Hz, H-8), 3.18 (dd, $J = 14$ Hz and 8.6 Hz, H-7) and 3.07 (dd, $J = 14$ Hz and 4.3 Hz, H-7); ^{13}C NMR (CD_3OD , 125 MHz): δ c 172.3 (C-9), 167.2 (C-9'), 148.3 (C-3 and C-5'), 146.5 (C-4'), 145.4 (C-7'), 144.7 (C-4), 127.9 (C-7), 126.2 (C-1'), 121.9 (C-6), 120.5 (C-2'), 115.2 (C-5 and C-3'), 115.0 (C-8'), 112.9 (C-6'), 73.3 (C-8) and 37.5 (C-7).

The spectral data obtained was identical to that reported data (Akoury, 2017; Serrano et al., 2021). Both the compounds were evaluated for antimycobacterial efficacy by CRI assay against both the strains including H37Rv and MDR as depicted in Table 3. The results show both compounds exhibited good antitubercular efficacy at 15–32 $\mu\text{g/mL}$ against both the standard and MDR strains.

Table 1. Antimycobacterial activity of crude *P. abrotanoides* extracts/fractions against H37Rv and MDR strain of *M. tuberculosis*.

Extracts/fractions	MIC values ($\mu\text{g/mL}$)	
	H37Rv	MDR strain
<i>P. abrotanoides</i> hexane (Hex) fraction	375	>1000
<i>P. abrotanoides</i> dichloromethane (DCM) fraction	187.5	250
<i>P. abrotanoides</i> ethyl acetate (EtOAc) fraction	125	125
<i>P. abrotanoides</i> methanolic (MeOH) fraction	250	500
<i>P. abrotanoides</i> aqueous (Aq) extract	500	500
Rifampicin	0.08	1

Table 2. Antimycobacterial activity of ethyl acetate fractions of *P. abrotanoides* against *M. tuberculosis* H37RV, and clinical isolates.

Fractions	MIC values ($\mu\text{g/mL}$)	
	H37Rv	MDR strain
Fr 1	125	250
Fr 2	62.5	125
Fr 3	31.25	62.5
Fr 4	125	125
Fr 5	62.5	250
Fr 6	31.25	31.25
Fr 7	250	500
Fr 8	500	>1000
Rifampicin	0.08	1

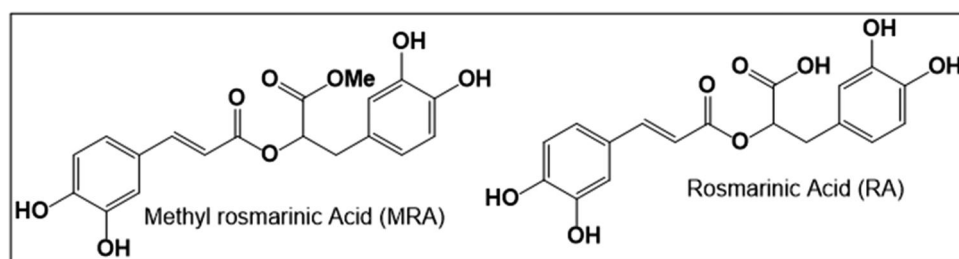


Figure 1. The chemical structure of isolated compounds from *P. abrotanoides*.

Table 3. Antimycobacterial activity of isolated compound from *P. abrotanoides* against *M. tuberculosis* H37RV, and clinical isolates.

Pure compounds	MIC values ($\mu\text{g}/\text{mL}$)	
	H37Rv	MDR strain
Methyl rosmarinic acid	31.25	31.25
Rosmarinic acid	15.62	31.25
Rifampicin	0.08	1

Due to the less quantity of the isolated pure compound, further *in-vivo* study could not be performed. But to understand the mechanistic way, docking studies were performed. To explore the target of the compounds and provide insights into why they showed disparate antimycobacterial effects, molecular docking was carried out on the various potential protein of *M. tuberculosis*. Both rosmarinic acid and methyl rosmarinate have been reported to have several targets in humans for various diseases such as cancer, diabetes, etc. Some of the targets of rosmarinate in humans for various types of cancer include cAMP-dependant protein kinase, Human Abl kinase, PI3 kinase, epidermal growth factor receptor, etc (Kang et al., 2003; Lata & Akif, 2021). To identify the probable target protein for rosmarinic acid and methyl rosmarinate in *M. tuberculosis*, docking analysis was performed with 22 known drug targets. Those targets were selected based on the potential of the proteins in *M. tuberculosis*.

3.2. Identification of potential *M. tuberculosis* protein targets for rosmarinic acid and methyl rosmarinic acid using docking analysis

The target rosmarinic acid showed the best binding affinity with Rv2623 of *Mycobacterium tuberculosis* (PDB:3CIS), i.e. -9.5 kcal/mol. However, rosmarinic acid had the highest number of *H*-bond interactions with a crystal structure of the *seca* protein translocation ATPase from *Mycobacterium tuberculosis* complex with adpbs' (PDB:1NKT), i.e. 12 (Table 4); 3D interaction is presented in Figure 2. Similarly, methyl-rosmarinic acid had the highest binding affinity with *Mycobacterium tuberculosis* lipoamide dehydrogenase (PDB:3II4) with the best binding energy of -8.9 kcal/mol via 3 *H*-bonds with Glu185, Cys41, and Ala141 (Table 5); 3D interaction is presented in Figure 2. However, methyl-rosmarinic acid had the highest *H*-bond interactions, i.e. 9 with Tyr841, Thr1044, Gln1061, Arg930, Asn928, and Ser1047. However, the rosmarinic acid and methyl-rosmarinic acid were non-interacting with the amino acid residues interacted by the co-crystallized ligand.

3.3. MD Simulation studies for the selection of the putative *Mtb* target of rosmarinic acid and its analogs

Docking results indicated that rosmarinic acid might bind comparatively more tightly with Mtb Rv2623 (Binding energy = -9.5 kcal/mol) than lipoamide dehydrogenase (Binding energy = -9.2 kcal/mol); although there was no significant difference in their respective binding energy scores. By contrast, rosmarinic acid methyl ester was revealed to bind comparatively more tightly with Mtb lipoamide dehydrogenase (Binding energy = -8.9 kcal/mol) than Rv2623 (Binding energy = -7.9 kcal/mol). It was our curiosity to address the question: which one of these two protein-ligand complexes is comparatively more stable energetically and thermodynamically, and thus, the possible target for rosmarinic acid? In addition, it was also expected to delineate the possible target for other similar ligands. Therefore, the equilibrated systems of these Mtb protein-ligand complexes were subjected to a production run of 100 ns, in each case, to see whether the predicted protein-ligand complexes were stable during the simulation time of 100 ns (Ponnusamy et al., 2023). Figures 3A and 4A illustrate the root mean square deviation (RMSD) plots obtained from the MD trajectory of the two protein-ligand complexes obtained after a 100 ns production run. As evident from Figures 3A and 4A, both the Mtb Rv2623-rosmarinic acid and Mtb lipoamide dehydrogenase-rosmarinic acid methyl ester complexes attained the equilibrium protein-backbone RMSD values below 0.3 nm. The RMSD values indicated that both complexes were stable throughout the simulation. Figures 3B and 4B show the plots of the intermolecular hydrogen bonds in the case of rosmarinic acid -Mtb RV2623 and rosmarinic acid methyl ester -Mtb lipoamide dehydrogenase, respectively, as observed during 100 ns of simulations. Throughout the MD simulation, the number of hydrogen bonds between protein and ligand converged to three. Figures 3C and 4C depict the location of the binding site and an enlarged view of the overlay of the starting and final confirmation of the two ligands with their respective proteins. As evident, there was a minor change in the conformation of rosmarinic acid and rosmarinic acid methyl ester when bound with their respective proteins. Figure 3D and E depict stable rosmarinic acid conformation (thick stick model) with surrounding amino acid residues, shown as surface view and thin stick model, respectively. The main chain ester keto group formed a hydrogen bond with backbone NH of Val277. The 3,4-hydroxyphenyl ring participated in hydrogen bonding with Asp167 (side chain

Table 4. Docking results for rosmarinic acid.

S. No.	PDB	Binding energy (kcal/mol)	Number of hydrogen bonds	Hydrogen bond residues
1	1F8M	-6.8	4	Trp17, Val26, Trp23,Lys24
2	1KNC	-6.2	3	Asn109, Ile106, Asn105
3	1M4I	-7.3	6	Gln93, Gly92, Arg94, Leu95, Val96, Val84
4	1NKT	-8.9	12	Gln80, Asp501, Asn499, Thr108, Arg137, Lys107,Glu105, Gly106, Arg490
5	1UZL	-7.3	6	Gln93, Gly92, Arg94, Leu95, Val96, Val84
6	1XFC	-6.8	5	Gly230, Ser213, His172, Tyr364, Asn184
7	1XKF	-7.4	4	His31, Arg101, Thr13
8	2A87	-8.1	5	Gly50, Arg253, Ser22, Val93
9	2CCA	-8.4	3	His116, Asn602, Arg119
10	2FUM	-7.2	6	Val95, Asp156, Asn143
11	2O7G	-7	7	Ser72, Arg71, Trp77, Ser69, Ala70
12	2PZI	-8.1	5	Ile292, Glu280, Asn281, Lys181
13	2QX1	-7.4	7	Asn65, Arg61, Val8, Arg12,Thr289
14	2WGE	-6.7	3	Pro147, Met114, Gly117
15	3C3W	-6.7	3	Ser186, Thr82, Gly60
16	3CIS	-9.5	6	Ala195, Gly262, Gly165, Gly268, Gly278, Asp167
17	3E05	-6.6	6	Thr232, Thr352, Val351, Thr355, Ser325
18	3II4	-9.2	2	Ala141, Tyr161
19	3LWB	-8.4	3	Leu117, Arg316
20	3PTY	-8.1	5	Ser1047, Ala922, Thr1044, Val1045
21	4HCX	-7.5	2	Val116, Glu113
22	4V1H	-6.3	0	-

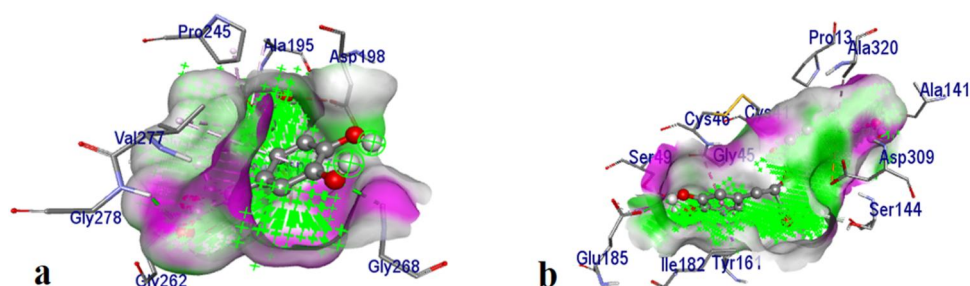


Figure 2. Interaction of (a) rosmarinic acid and with Rv2623 of *mycobacterium tuberculosis* (PDB: 3CIS) and (b) rosmarinic acid methyl ester with mycobacterial lipamide dehydrogenase (PDB: 3II4).the green cross (X) represents the pocket of the protein where the ligand was observed to be embedded. In the above figure, 'ball and stick' represents the ligand whereas 'lines' present the amino acids of respective targets. The increase in the color of the green and purple are directly proportional to the strength of the H-bond acceptor and donor respectively.

Table 5. Docking results for methyl-rosmarinic acid.

S. No.	PDB ID	Binding energy (kcal/mol)	Number of hydrogen bonds	Hydrogen bond residues
1	1F8M	-6.6	3	Arg28,Val26, Trp23
2	1KNC	-5.8	2	Glu138
3	1M4I	-7.0	6	Trp181, Ser119, Glu82, Gly83, Ser117
4	1NKT	-6.7	4	Arg638, Asp216, Gln632
5	1UZL	-7.0	3	Val81, Trp181, Asp40
6	1XFC	-6.3	4	Asp244, Ser237, Asp354, Gly345
7	1XKF	-8.3	6	Arg101, His31, Asp43, Arg109, Asp32
8	2A87	-6.4	3	Thr299, Ser303, Thr293
9	2CCA	-7.8	3	Arg114, Glu217, Val586
10	2FUM	-7.3	4	Glu93, Tyr94, Val95, Gly97
11	2O7G	-6.1	2	Arg67, Arg71
12	2PZI	-8.1	4	Ala296, Asp293, Leu183
13	2QX1	-7.6	6	Val8, Arg12, Asp268, His271
14	2WGE	-7.8	3	Ile317, His345, Phe402
15	3C3W	-7.1	6	Lys182, Arg56, Gly164, Asn167, Gln199
16	3CIS	-7.9	7	Arg127, Gly120, Ser131, Ser121, Gly117, Ala43, Ile14
17	3E05	-6.6	3	Lys229, Thr232, Val351
18	3II4	-8.9	3	Glu185, Cys41, Ala141
19	3LWB	-8.3	4	Ser341, Tyr277, His118, Arg316
20	3PTY	-8.1	9	Tyr841, Thr1044, Gln1061,Arg930, Asn928, Ser1047
21	4HCX	-7.5	5	Asn205, Gln344, Val116, Glu113, Thr295
22	4V1H	-6.1	2	Thr60

carboxylate), while another 3,4-dihydroxyphenyl ring participated in hydrogen bonding with Asp198 (side chain carboxylate) and pi-stacking contact with Arg266 (guanidine fragment). The carboxylate group of rosmarinic acid formed hydrogen bonds with Arg264 and Gly275. Similarly,

Meanwhile, Figure 4D and E depict the stable conformation (thick stick model) with surrounding amino acid residues surface view and thin stick model, respectively. The main chain ester keto formed a hydrogen bond with the backbone NH of Cys46. The two H-bond interactions of rosmarinic acid

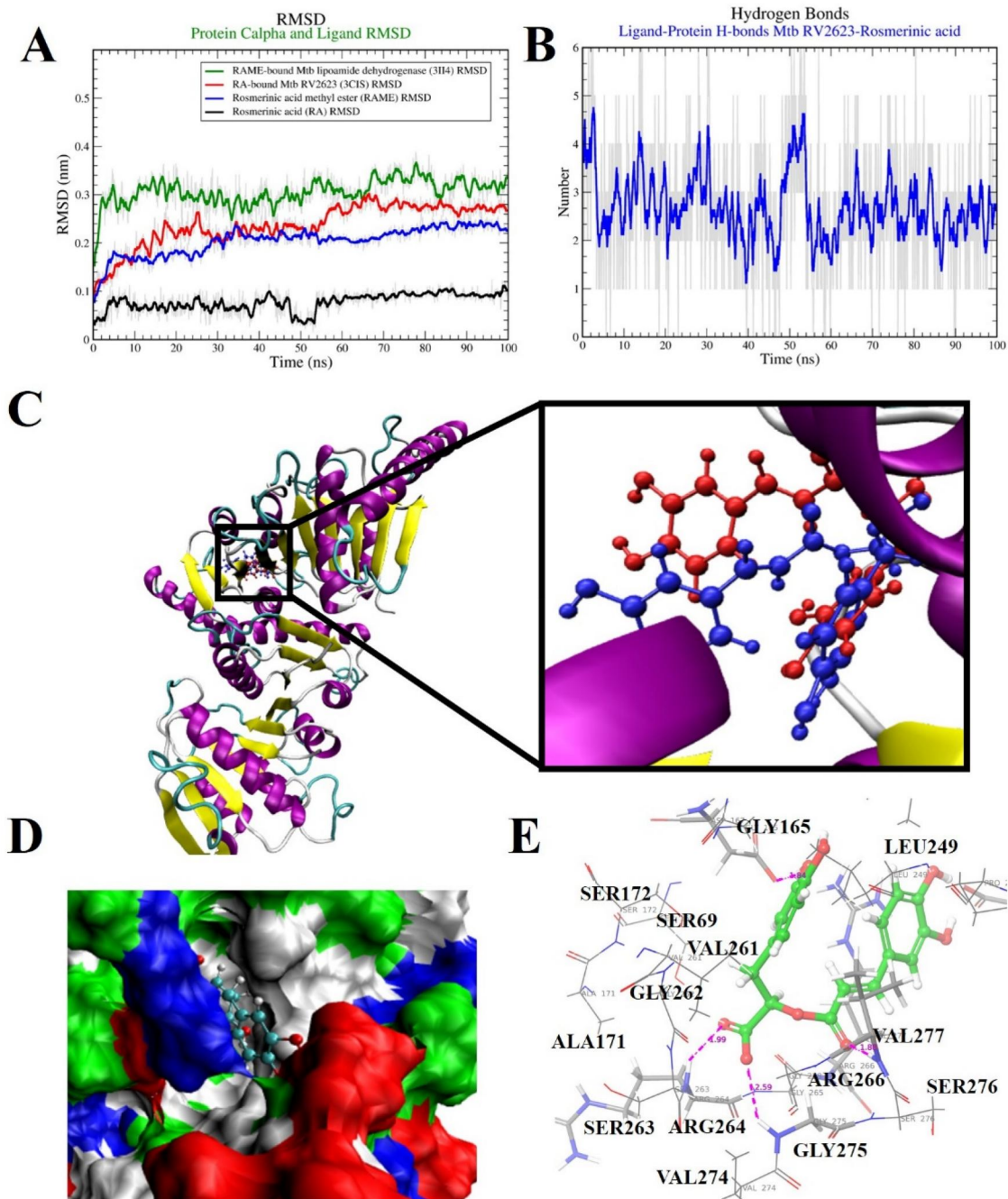


Figure 3. Results from the MD simulation of the Mtb RV2623 – rosmarinic acid complex. (A) The protein C- α RMSD from two MD simulations. (B) The hydrogen bond plot between rosmarinic acid and Mtb RV2623 during 100 ns of MD simulation. (C) The location of the binding site and enlarged view of overlay of the starting and final conformation of rosmarinic acid with Mtb RV2623, (D and E) rosmarinic acid conformation (thick stick model) with surrounding amino acid residues surface view and thin stick model, respectively.

methyl ester with protein residues Cys46 and Ser49 were observed. The 3,4-dihydroxyphenyl ring participated in hydrogen bonding with the side chain hydroxyl of Ser49.

4. Conclusion

In conclusion, this study investigated the antimycobacterial potential of compounds isolated from *P. abrotanoides* against *M. tuberculosis*. The bioactive compounds, Rosmarinic acid and Rosmarinic acid methyl ester were successfully isolated from *P. abrotanoides* and exhibited promising antimycobacterial

activity against both drug-sensitive and MDR strains of *M. tuberculosis*. The results of this study contribute to the growing body of research exploring natural compounds as potential sources of novel antimycobacterial agents. Rosmarinic acid and Rosmarinic acid methyl ester demonstrated significant inhibitory effects at relatively low concentrations, highlighting their potential for further development as anti-tuberculosis agents. Additionally, the docking studies provided insights into the possible binding interactions of these compounds with specific *M. tuberculosis* proteins, shedding light on their mechanisms of action. According to the molecular docking

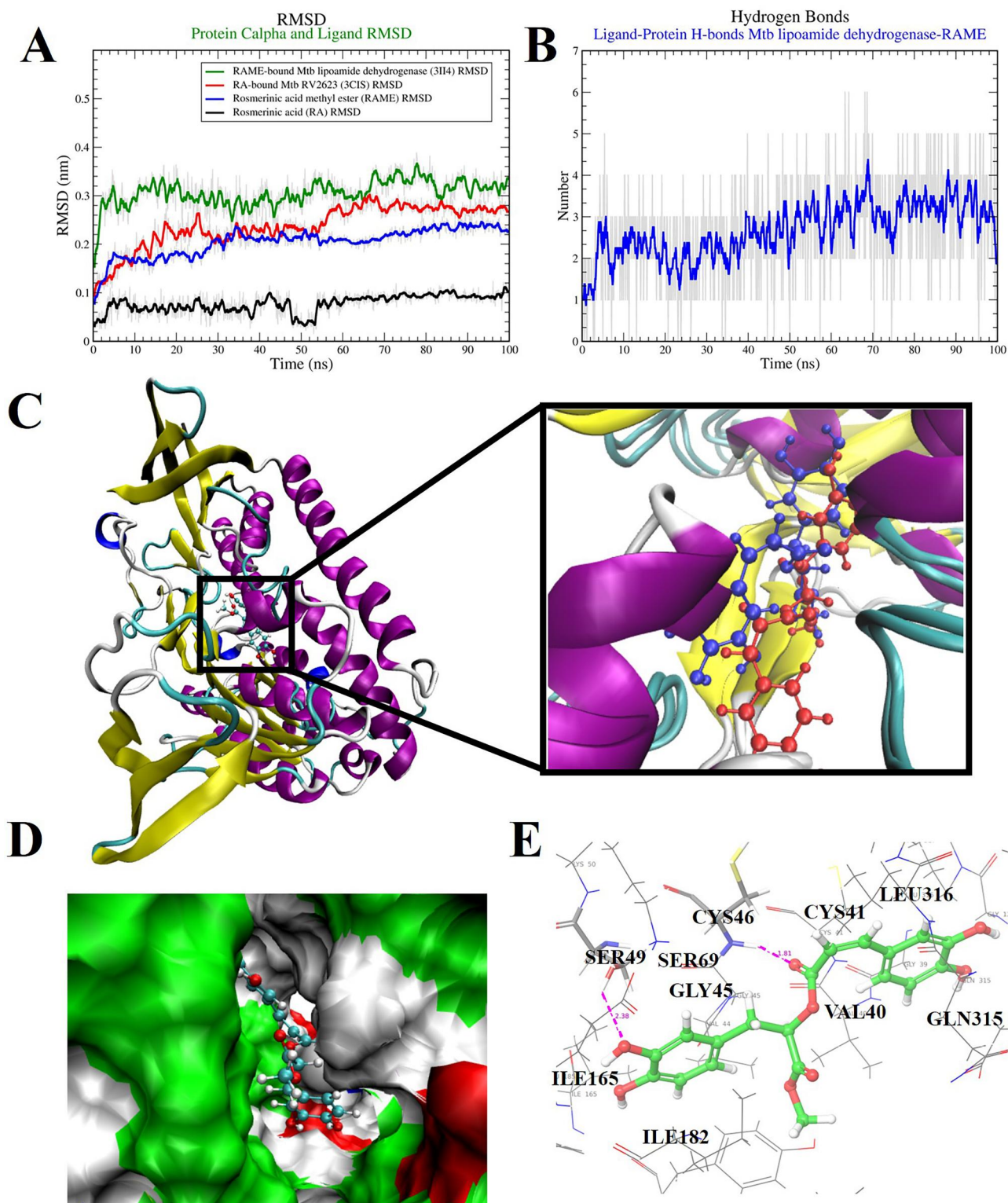


Figure 4. Results from the MD simulation of the Mtb lipamide dehydrogenase – rosmarinic acid methyl ester complex. (A) The protein C- α RMSD from two MD simulations. (B) The hydrogen bond plot between rosmarinic acid methyl ester and Mtb lipamide dehydrogenase during 100 ns of MD simulation. (C) The location of the binding site and enlarged view of overlay of the starting and final conformation of rosmarinic acid methyl ester with Mtb lipamide dehydrogenase, (D and E) rosmarinic acid methyl ester conformation (thick stick model) with surrounding amino acid residues surface view and thin stick model, respectively.

and MD simulations study, lipamide dehydrogenase and Rv2623 proteins were found to be potential Mtb targets of Rosmarinic acid and Rosmarinic acid methyl ester, respectively. However, it should be noted that while *in vitro* assays and computational simulations are valuable tools for preliminary

evaluation, further studies are required to validate the potential of rosmarinic acid and rosmarinic acid methyl ester as anti-tuberculosis agents. *In vivo*, experiments and clinical trials are necessary to determine their efficacy, safety, and pharmacokinetic profiles.

Acknowledgment

The authors thank Sarman Joshi of AIIMS, New Delhi, S. Kitchlu of IIM (CSIR), Jammu, and Dr. Sabari Ghosal of Amity University Noida, Uttar Pradesh for providing facilities to carry out this work.

Disclosure statement

All the authors of this manuscript declare that they do not have any conflict of interest by any financial and non-financial means.

Funding

Yadu Nandan Dey and Kuldeep K. Roy also wish to thank Science and Engineering Research Board, Department of Science and Technology for providing necessary facilities for the projects through Grant Number SRG/2021/001631 and SRG/2021/001734, respectively.

ORCID

Nandan Sarkar  <http://orcid.org/0000-0003-3032-4527>

Pukar Khanal  <http://orcid.org/0000-0002-8187-2120>

Ravi Rawat  <http://orcid.org/0000-0001-6510-1046>

Yadu Nandan Dey  <http://orcid.org/0000-0003-4016-4379>

Kuldeep K. Roy  <http://orcid.org/0000-0001-9623-0617>

Reference

- Akoury, E. (2017). Isolation and structural elucidation of rosmarinic acid by nuclear magnetic resonance spectroscopy. *Asian Journal of Green Chemistry*, 2, 17–23.
- Alizadeh, Z., Farimani, M. M., Parisi, V., Marzocco, S., Ebrahimi, S. N., & De Tommasi, N. (2021). Nor-abietane diterpenoids from *Perovskia abrotanoides* Roots with anti-inflammatory potential. *Journal of Natural Products*, 84(4), 1185–1197. <https://doi.org/10.1021/acs.jnatprod.0c01256>
- Beikmohammadi, M. (2012). The evaluation of medicinal properties of *Perovskia abrotanoides* Karel. *Middle-East Journal of Scientific Research*, 11(2), 189–193.
- Benjamin, I., Udoikono, A. D., Louis, H., Agwamba, E. C., Unimuke, T. O., Owen, A. E., & Adeyinka, A. S. (2022). Antimalarial potential of naphthalene-sulfonic acid derivatives: Molecular electronic properties, vibrational assignments, and *in-silico* molecular docking studies. *Journal of Molecular Structure*, 1264, 133298. <https://doi.org/10.1016/j.molstruc.2022.133298>
- Bhattacharya, K., Khanal, P., Patil, V. S., Dwivedi, P. S. R., Chanu, N. R., Chaudhary, R. K., Deka, S., & Chakraborty, A. (2023). Computational pharmacology profiling of borapetoside C against melanoma. *Journal of Biomolecular Structure & Dynamics*, 1–16. <https://doi.org/10.1080/07391102.2023.2213333>
- Bloom, B. R., Atun, R., & Cohen, T. (2017). Tuberculosis. In K. K. Holmes, S. Bertozzi, B. R. Bloom (Eds.), *Major infectious diseases*, 3rd ed. The International Bank for Reconstruction and Development/The World Bank. Nov 3. Chapter 11.
- Chattaraj, B., Khanal, P., Nandi, A., Das, A., Sharma, A., Mitra, S., & Dey, Y. N. (2023). Network pharmacology and molecular modelling study of *Enhydra fluctuans* for the prediction of the molecular mechanisms involved in the amelioration of nephrolithiasis. *Journal of Biomolecular Structure & Dynamics*, 1–11. <https://doi.org/10.1080/07391102.2023.2189476>
- Chou, T. H., Chen, J. J., Peng, C. F., Cheng, M. J., & Chen, I. S. (2011). New flavanones from the leaves of *Cryptocarya chinensis* and their antituberculosis activity. *Chemistry & Biodiversity*, 8(11), 2015–2024. <https://doi.org/10.1002/cbdv.201000367>
- Eno, E. A., Cheng, C. R., Louis, H., Gber, T. E., Emori, W., Ita, I. A., Unimuke, T. O., Ling, L., Adalikwu, S. A., Agwamba, E. C., & Adeyinka, A. S. (2022). Investigation on the molecular, electronic and spectroscopic properties of rosmarinic acid: An intuition from an experimental and computational perspective. *Journal of Biomolecular Structure & Dynamics*, 13, 1–15. <https://doi.org/10.1080/07391102.2022.2154841>
- Fachel, F. N. S., Schuh, R. S., Veras, K. S., Bassani, V. L., Koester, L. S., Henriques, A. T., Braganhol, E., & Teixeira, H. F. (2019). An overview of the neuroprotective potential of rosmarinic acid and its association with nanotechnology-based delivery systems: A novel approach to treating neurodegenerative disorders. *Neurochemistry International*, 122, 47–58. <https://doi.org/10.1016/j.neuint.2018.11.003>
- Fazel Nabavi, S., Carlo Tenore, G., Daglia, M., Tundis, R., Rosa Loizzo, M., & Mohammad Nabavi, S. (2015). The cellular protective effects of Rosmarinic acid: From bench to bedside. *Current Neurovascular Research*, 12(1), 98–105. <https://doi.org/10.2174/1567202612666150109113638>
- Fernandes, G. F., Campos, D. L., Da Silva, I. C., Prates, J. L., Pavan, A. R., Pavan, F. R., & Dos Santos, J. L. (2021). Benzofuroxan derivatives as potent agents against multidrug-resistant *Mycobacterium tuberculosis*. *ChemMedChem*, 16(8), 1268–1282. <https://doi.org/10.1002/cmdc.202000899>
- Humphrey, W., Dalke, A., & Schulten, K. (1996). VMD: Visual molecular dynamics. *Journal of Molecular Graphics*, 14(1), 33–38. [https://doi.org/10.1016/0263-7855\(96\)00018-5](https://doi.org/10.1016/0263-7855(96)00018-5)
- Ignacimuthu, S., & Shanmugam, N. (2010). Antimycobacterial activity of two natural alkaloids, vasicine acetate and 2-acetyl benzylamine, isolated from Indian shrub *Adhatodavasica* Ness. leaves. *Journal of Biosciences*, 35(4), 565–570. <https://doi.org/10.1007/s12038-010-0065-8>
- Jiang, Z., Gao, W., & Huang, L. (2019). Tanshinones, critical pharmacological components in *Salvia miltiorrhiza*. *Frontiers in Pharmacology*, 10, 202. <https://doi.org/10.3389/fphar.2019.00202>
- Kang, M. A., Yun, S. Y., & Won, J. (2003). Rosmarinic acid inhibits Ca²⁺-dependent pathways of T-cell antigen receptor-mediated signaling by inhibiting the PLC- γ 1 and Itk activity. *Blood*, 101(9), 3534–3542. <https://doi.org/10.1182/blood-2002-07-1992>
- Khanal, P., Patil, B. M., Chand, J., & Naaz, Y. (2020). Anthraquinone derivatives as an immune booster and their therapeutic option against COVID-19. *Natural Products and Bioprospecting*, 10(5), 325–335. <https://doi.org/10.1007/s13659-020-00260-2>
- Khanal, P., Zargari, F., Far, B. F., Kumar, D., R, M., Mahdi, Y. K., Jubair, N. K., Saraf, S. K., Bansal, P., Singh, R., Selvaraja, M., & Dey, Y. N. (2021). Integration of system biology tools to investigate huperzine A as an anti-alzheimer agent. *Frontiers in Pharmacology*, 12, 785964. <https://doi.org/10.3389/fphar.2021.785964>
- Kohl, J., Kolnaar, R., & Ravensberg, W. J. (2019). Mode of action of microbial biological control agents against plant diseases: Relevance beyond efficacy. *Frontiers in Plant Science*, 10, 845. <https://doi.org/10.3389/fpls.2019.00845>
- Kumari, M., Singh, R., & Subbarao, N. (2022). Exploring the interaction mechanism between potential inhibitor and multi-target Mur enzymes of mycobacterium tuberculosis using molecular docking, molecular dynamics simulation, principal component analysis, free energy landscape, dynamic cross-correlation matrices, vector movements, and binding free energy calculation. *Journal of Biomolecular Structure & Dynamics*, 40(24), 13497–13526. <https://doi.org/10.1080/07391102.2021.1989040>
- Lata, S., & Akif, M. (2021). Structure-based identification of natural compound inhibitor against *M. tuberculosis* thioredoxin reductase: Insight from molecular docking and dynamics simulation. *Journal of Biomolecular Structure & Dynamics*, 39(12), 4480–4489. <https://doi.org/10.1080/07391102.2020.1778530>
- Mahboubi, M., & Kazempour, N. (2009). The antimicrobial activity of essential oil from *Perovskia Abrotanoides* Karel and its main components. *Indian Journal of Pharmaceutical Sciences*, 71(3), 343–347. <https://doi.org/10.4103/0250-474X.56016>
- Manicum, A. L., Louis, H., Agwamba, E. C., Chima, C. M., Nzondomyo, W. J., & Sithole, S. (2023). Acetylacetone and imidazole coordinated Re (I) tricarbonyl complexes: Experimental, DFT studies, and molecular docking approach. *Chemical Physics Impact*, 6, 100165. <https://doi.org/10.1016/j.chphi.2023.100165>
- Moghaddas, E., Khamesipour, A., Mohebbi, M., & Fata, A. (2017). Iranian native plants on treatment of cutaneous leishmaniasis: A narrative review. *Iranian Journal of Parasitology*, 12(3), 312.
- Nandi, A., Das, A., Dey, Y. N., & Roy, K. K. (2023). The abundant phytocannabinoids in rheumatoid arthritis: Therapeutic targets and molecular

- processes identified using integrated bioinformatics and network pharmacology. *Life (Basel, Switzerland)*, 13(3), 700. <https://doi.org/10.3390/life13030700>
- Owen, A. E., Louis, H., Agwamba, E. C., Udoikono, A. D., & Manicum, A. L. (2023). Antihypotensive potency of p-synephrine: Spectral analysis, molecular properties and molecular docking investigation. *Journal of Molecular Structure*, 1273, 134233. <https://doi.org/10.1016/j.molstruc.2022.134233>
- Patil, P. P., Kumar, P., Khanal, P., Patil, V. S., Darasaguppe, H. R., Bhandare, V. V., Bhatkande, A., Shukla, S., Joshi, R. K., Patil, B. M., & Roy, S. (2023). Computational and experimental pharmacology to decode the efficacy of *Theobroma cacao* L. against doxorubicin-induced organ toxicity in EAC-mediated solid tumor-induced mice. *Frontiers in Pharmacology*, 14, 1174867. <https://doi.org/10.3389/fphar.2023.1174867>
- Ponnusamy, N., Pillai, G., & Arumugam, M. (2023). Computational investigation of phytochemicals identified from medicinal plant extracts against tuberculosis. *Journal of Biomolecular Structure & Dynamics*, 11, 1–14. <https://doi.org/10.1080/07391102.2023.2213341>
- Pronk, S., Pall, S., Schulz, R., Larsson, P., Bjelkmar, P., Apostolov, R., Shirts, M. R., Smith, J. C., Kasson, P. M., van der Spoel, D., Hess, B., & Lindahl, E. (2013). GROMACS 4.5: A high-throughput and highly parallel open-source molecular simulation toolkit. *Bioinformatics (Oxford, England)*, 29(7), 845–854. <https://doi.org/10.1093/bioinformatics/btt055>
- Rawat, R., Kant, K., Kumar, A., Bhati, K., & Verma, S. M. (2021). HeroMDAnalysis: An automagical tool for GROMACS based molecular dynamics simulation analysis. *Future Medicinal Chemistry*, 13(5), 447–456. <https://doi.org/10.4155/fmc-2020-0191>
- Sarkar, N., Saha, B., Singh, S., & Ghosal, S. (2018). *Tropidia curculioides*: Secondary metabolites and derivatives with antimycobacterial and leishmanicidal activity. *Pharmacognosy Magazine*, 14(59), 535. https://doi.org/10.4103/pm.pm_196_18
- Sedano-Partida, M. D., dos Santos, K. P., Sala-Carvalho, W. R., Silva-Luz, C. L., & Furlan, C. M. (2020). Anti-HIV-1 and antibacterial potential of *Hyptisradicans* (Pohl) Harley & JFB Pastore and *Hyptismultibracteata* Benth. (Lamiaceae). *Journal of Herbal Medicine*, 20, 100328. <https://doi.org/10.1016/j.hermed.2019.100328>
- Serrano, C. A., Villena, G. K., & Rodríguez, E. F. (2021). Phytochemical profile and rosmarinic acid purification from two Peruvian *lepechinia* Willd. species (Salviinae, Mentheae, Lamiaceae). *Scientific Reports*, 11(1), 7260. <https://doi.org/10.1038/s41598-021-86692-3>
- Van Der Spoel, D., Lindahl, E., Hess, B., Groenhof, G., Mark, A. E., & Berendsen, H. J. (2005). GROMACS: Fast, flexible, and free. *Journal of Computational Chemistry*, 26(16), 1701–1718. <https://doi.org/10.1002/jcc.20291>
- Wei, K., Louis, H., Emori, W., Idante, P. S., Agwamba, E. C., Cheng, C. R., Eno, E. A., & Unimuke, T. O. (2022). Antispasmodic activity of carnosic acid extracted from *Rosmarinus officinalis*: Isolation, spectroscopic characterization, DFT studies, and *in-silico* molecular docking investigations. *Journal of Molecular Structure*, 1260, 132795. <https://doi.org/10.1016/j.molstruc.2022.132795>
- Zhang, Q., Sun, J., Wang, Y., He, W., Wang, L., Zheng, Y., Wu, J., Zhang, Y., & Jiang, X. (2017). Antimycobacterial and anti-inflammatory mechanisms of baicalin via induced autophagy in macrophages infected with *Mycobacterium tuberculosis*. *Frontiers in Microbiology*, 8, 2142.